ARTICLE

Microstructure evolution and enhanced mechanical properties of hot rolled Mg–3Al–Zn alloy with the addition of Al and Si as a eutectic alloy

Liuwei Zheng and Kaibo Nie
Shanxi Key Laboratory of Advanced Magnesium-based Materials, Taiyuan 030024, China; and College of Materials Science and Engineering, Taiyuan University of Technology, Taiyuan 030024, China

Huihui Nie
Shanxi Key Laboratory of Advanced Magnesium-based Materials, Taiyuan 030024, China; College of Materials Science and Engineering, Taiyuan University of Technology, Taiyuan 030024, China; and Shanxi Institute of Energy, Taiyuan 030600, China

Wanggang Zhang and Wei Liang[a)]
Shanxi Key Laboratory of Advanced Magnesium-based Materials, Taiyuan 030024, China; and College of Materials Science and Engineering, Taiyuan University of Technology, Taiyuan 030024, China

Yide Wang
Shanxi Key Laboratory of Advanced Magnesium-based Materials, Taiyuan 030024, China; and Taiyuan Iron and Steel (Group) Co., LTD, Taiyuan 030003, China

(Received 16 February 2017; accepted 1 June 2017)

Mg–3Al–Zn alloy with the addition of Al and Si as a eutectic alloy was subjected to conventional hot rolling. The corresponding mechanical properties, microstructure evolution, and dynamic recrystallization mechanism were investigated by optical microscope, scanning electron microscope, electron backscattered diffraction (EBSD), and tensile tests. The experimental results indicated that the Mg–3(Al–Si)–Zn alloy had a microstructure refinement, thus rendering an enhanced mechanical properties in comparison with the Mg–3Al–Zn alloy. The refined Mg_2Si particles could act as potential nucleation sites for recrystallization in as-rolled Mg–3(Al–Si)–Zn alloy sheets, which resulted in more completely recrystallized regions through particle stimulated nucleation and a weakened basal texture compared to Mg–3Al–Zn alloy. The improvement in the tensile strength of the as-rolled Mg–3(Al–Si)–Zn alloy can be attributed to grain refinement and second phase strengthening caused by the refined Mg_2Si particles.

I. INTRODUCTION

Wrought magnesium alloys formed by plastic deformation, such as rolling, extrusion, and forging, have the potential for a superior combination of strength and ductility compared to cast magnesium alloys. However, the engineering applications of wrought magnesium alloys are still somewhat limited because of their relatively low strength and ductility.[1] Alloying is one of the most effective methods to improve strength in magnesium alloys, and it could be used to generate a strengthening phase and to promote grain refinement. It has been reported that adding rare earth elements, such as Y,[2] Gd,[3] and Nd,[4] to magnesium alloys can improve their strength and prompt texture modification. Although the rare earth precipitated phase helps to improve strength, in most cases, the ductility deteriorates, and the production cost of the magnesium alloy significantly increases.[2,5] This reduces the commercial applications of magnesium alloys. Therefore, the addition of a low-cost element that could increase both the strength and ductility of magnesium alloys will lead to more applications for the materials. The AZ series alloys, which mainly contain Al and Zn alloy elements, are low cost materials with relatively appropriate ambient temperature mechanical properties, and they have attracted attention for their ability to improve strength and ductility and to adapt to much higher performance structural applications.[1,6,7]

Previous studies[8,9] have suggested that the addition of Si to an AZ series alloy can result in strengthening effects, especially at elevated temperatures because of the formation of a Mg_2Si phase with a high melting point (1085 °C) and high elastic modulus (120 GPa). However, coarse Mg_2Si phases with a Chinese script shape are prone to form at lower solidification rates, and these phases are detrimental to the mechanical properties of the alloy,[10,11] which could seriously restrict plastic processing and further strength improvements of the magnesium

Contributing Editor: Jürgen Eckert
[a)]Address all correspondence to this author.
e-mail: liangwei@tyut.edu.cn
DOI: 10.1557/jmr.2017.248

alloys. To obtain Mg_2Si phases with desirable shapes, various methods, such as adding modifying elements (e.g., strontium[12]), and using rapid solidification, powder metallurgy,[13] and solution heat treatment,[14] have been used. However, the refinement and distribution of the Mg_2Si phase created by these processing techniques is still unsatisfactory. The refinement of the Mg_2Si phase is critical for enhancement of the mechanical properties of AZ series alloys with Si addition. In our previous study,[15] adding Al and Si as a eutectic alloy into an Mg–Li alloy and combining the hot rolling process dramatically improved the tensile strength. A tensile strength of ~390 MPa for the Mg–8Li–6(Al–Si) alloy was achieved compared to ~200 MPa for the Mg–8Li alloy, and the significant improvement in the mechanical strength can be attributed to grain refinement and fine Mg_2Si precipitated particles. Therefore, a proper addition method for Si, such as an Al–Si eutectic alloy, is expected to be an effective way to acquire enhanced mechanical properties for AZ series alloys.

In addition, plastic deformation results in grain refinement and is a useful method to enhance the mechanical properties of magnesium alloys. There are several ways to achieve deformation strengthening, such as conventional extrusion,[2,16] forging,[17] rolling,[1,18,19] and severe plastic deformation (SPD). According to the Hall–Petch[20] relationship, grain refinement induced by dynamic recrystallization (DRX) during plastic deformation plays a critical role in improving the mechanical properties of magnesium alloys. Accordingly, most studies focus on grain refinement to acquire finer grains, such as ultra-fine grains and even nano-grains, using SPD at high temperatures. SPD techniques, which include equal channel angular pressing (ECAP),[4] accumulative roll bonding (ARB)[21] and multidirectional forging (MDF),[7] can yield considerable grain refinement and improvement in mechanical properties. However, the ductility and plastic formability after SPD tend to be restricted, which limits the practical application value of SPD. Recently, Wu et al.[22] successfully created heterogeneous lamella microstructures combined with ultra-fine grains and coarse grains in metal Ti, and this metal exhibited superior strength and excellent ductility upon asymmetric rolling and partial recrystallization. This method may also apply to alloys, and persistently pursuing grain refinement may not be a particularly effective pathway for magnesium alloys.

Combining alloying and deformation strengthening could be the most effective approach to achieve high performance AZ series alloys. Thus, fragmentation of the coarse and hard to refined phases (e.g., Mg_2Si) through thermo–mechanical forming should be a focus of efforts to enhance the mechanical properties of AZ series alloys containing Si. In the present research, a suitable alloying method and thermo–mechanical processing, which brought about a duplex grain structure involving ultra-fine DRX grains and coarse grains and refined the Mg_2Si strengthening phase, were designed to produce AZ31 alloy sheets with better mechanical properties. The microstructure evolution and deformation mechanism were also investigated.

II. MATERIALS AND METHODS

The original materials used for this study were commercially pure Mg (99.99 wt%), Al (99.9 wt%), Zn (99.9 wt%), and Si (99.9 wt%). Al–Si eutectic alloys with 12.6 wt% Si were prepared in a copper crucible using a vacuum induction melting furnace. Before smelting the materials, the furnace was filled with argon gas after evacuation by a mechanical pump to $\sim 10^{-3}$ Pa. Four alloys with different compositions, Mg–3Al, Mg–3(Al–Si), Mg–3Al–Zn, and Mg–3(Al–Si)–Zn, as shown in Table I, were also prepared in a graphite crucible using a vacuum induction melting furnace. After complete melting and cooling in the furnace, the as-cast alloys were cut into cylinders 30 mm in diameter and 40 mm in length for the following hot extrusion. The hot extrusion was carried out at a pressing speed of 2 mm/s at 400 °C to create slabs with a section of 10 × 6 mm in width and thickness, respectively, after the prepared alloys were homogenized at 415 °C for 24 h followed by a water quench at 70 °C. The as-extruded alloys were reheated to 400 °C and held there for 30 min in the resistant furnace to prepare for a multi-pass hot rolling process. Then, the alloys were rolled into sheets with a thickness of 1.6 mm using multi-pass hot rolling with a thickness reduction of ~30% per rolling pass and a rolling speed of 60 mm/s. Owing to the relatively poor formability of the specimens at room temperature, the rolls were heated to 150 °C, and intermediate inter-pass reheating at 400 °C for 5 min was also used.

To study the evolution of the microstructure and texture of the prepared alloys in different states, optical microscopy (OM), scanning electron microscopy (SEM), energy dispersive system (EDS), X-ray diffraction (XRD), and electron backscattered diffraction (EBSD) were used. The samples for the microstructure and texture analyses were sectioned from the center area of the specimens with RD × TD and RD × ND cross sections.

TABLE I. Chemical compositions of prepared alloys (in wt%).

	Chemical composition (wt%)			
Alloy	Al	Si	Zn	Mg
Mg–3Al	2.98	...	...	Bal.
Mg–3(Al–Si)	2.61	0.38	...	Bal.
Mg–3Al–Zn	3.04	...	0.92	Bal.
Mg–3(Al–Si)–Zn	2.60	0.39	0.95	Bal.

The metallographic samples were prepared using a standard mechanical ground and polishing technique. The samples were then etched using an acetic picric solution, which was composed of 4.6 g of picric acid, 10 mL of acetic acid, 10 mL of distilled water, and 70 mL of ethanol. The metallographic microstructures were observed by a model DM450 optical microscope (Leica Microsystem GmbH, Wetzlar, Germany), and the average grain sizes were determined by analyzing the optical micrographs using the line-intercept method.[23] The phase composition was analyzed by XRD using a Siemens XRD D5000 (Siemens AG, Munich, Germany) operating at 40 kV and 20 mA (Cu K_α radiation). The EBSD samples were prepared via mechanical grinding and then placed in a solution of 10% perchloric acid and 90% ethanol using a voltage of 40 V for 30–50 s at a temperature of −20 °C. The EBSD measurements were performed on a Zeiss Supra 55VPFEG-SEM (Carl Zeiss AG, Oberkochen, Germany) using a voltage of 20 kV with a working distance of 20 mm, a tilt angle of 70° and a scan step of 0.5 μm.

To determine the mechanical properties of the alloys, the tensile specimens, with a gauge length of 25 mm, width of 3.5 mm, and thickness of 1.5 mm, were machined out of the rolled sheets along the rolling direction (RD). Tensile tests were performed on a CMT5205 electronic universal testing machine (MTS Systems, Shenzhen, China) at a cross-head speed of 0.5 mm/min at room temperature. A representative tensile stress–strain curve was selected, and the tensile test for each sample was conducted three times to ensure repeatability and consistency of the test results. The mechanical property values for yield strength, ultimate tensile strength (UTS), and elongation were obtained from the average of three test results.

III. RESULTS AND DISCUSSION

A. Microstructure evolution

To reveal the effect of adding the Al–Si eutectic alloy on the microstructure and texture characteristics of the AZ31 magnesium alloy, Mg–3Al–Zn and Mg–3(Al–Si)–Zn with four different processing statuses (i.e., as-cast, homogenized, as-extruded, and as-rolled) were specifically analyzed.

Figure 1 shows the XRD patterns of the as-cast and homogenized alloys. The patterns indicate that the $Mg_{17}Al_{12}$ phases were almost dissolved in the Mg matrix, whereas the Mg_2Si phases did not dissolve during the homogenization treatment. This was also confirmed by the optical microstructures of Mg–3Al–Zn and Mg–3(Al–Si)–Zn, which are shown in Fig. 2. The microstructures of both as-cast alloys consist of initial coarse grains with a grain size of ~150 μm and some small $Mg_{17}Al_{12}$ precipitates distributed along the grain boundaries and inner grains. The main difference is that the eutectic Mg_2Si phase in the Chinese script type form with a size of ~100 μm is observed in the Mg–3(Al–Si)–Zn alloy, as shown in

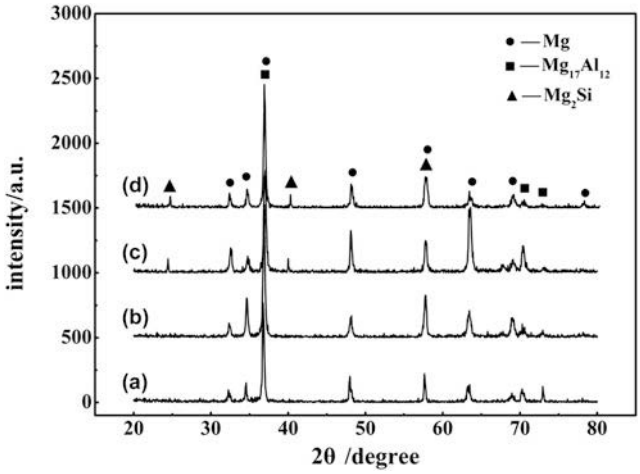

FIG. 1. XRD patterns of prepared Mg–3Al–Zn alloy [(a) as-cast and (b) homogenized] and Mg–3(Al–Si)–Zn alloy [(c) as-cast and (d) homogenized].

Figs. 2(a) and 2(b). After homogenization at 415 °C for 24 h, it was observed that the $Mg_{17}Al_{12}$ phase almost completely dissolved in both alloys. However, the Mg_2Si phase cannot be dissolved in the Mg–3(Al–Si)–Zn alloy, and this is related to its extremely low solid solubility[24] in Mg and its high melting point,[8] as shown in Figs. 3(c) and 3(d). The average grain size for the as-cast Mg–3Al–Zn and Mg–3(Al–Si)–Zn alloys varies slightly. The grains measured ~100 μm and ~120 μm, respectively, after the homogenization treatment.

The optical microstructures of the as-extruded Mg–3Al–Zn and Mg–3(Al–Si)–Zn alloys are shown in Fig. 3. The fine equiaxed grains in both Mg–3Al–Zn and Mg–3(Al–Si)–Zn alloys distribute along the extrusion direction in the form of an extrusion flow. The average grain size for the Mg–3Al–Zn and Mg–3(Al–Si)–Zn alloys decreases to ~30 μm and ~26 μm, respectively. The as-extruded Mg–3Al–Zn alloy exhibits a more uniform grain size distribution [Fig. 3(a)], whereas the Mg–3(Al–Si)–Zn alloy with the Al–Si eutectic shows some inhomogeneous microstructure and uneven grain size distribution. It was also found that the Mg_2Si phase with a distinct banding distribution along the extrusion direction in the as-extruded Mg–3(Al–Si)–Zn alloy was broken into small, blocky-shaped particles with an average size of ~5 μm. The fine grained regions around the broken, small Mg_2Si phases acted as band-like areas along the extrusion direction, whereas the grains far away from the broken, small Mg_2Si phases were coarse, as shown in Figs. 3(b) and 3(c). A similar case was reported by Fintová et al.[25] and Guo et al.[26] The formation of fine grained regions around the fractured, small Mg_2Si phases is mainly related to two aspects. Harder particles (with diameters ≥1 μm) in the magnesium alloys can promote DRX via lattice rotation during deformation.[27] Thus, the broken, small Mg_2Si phases could facilitate DRX through

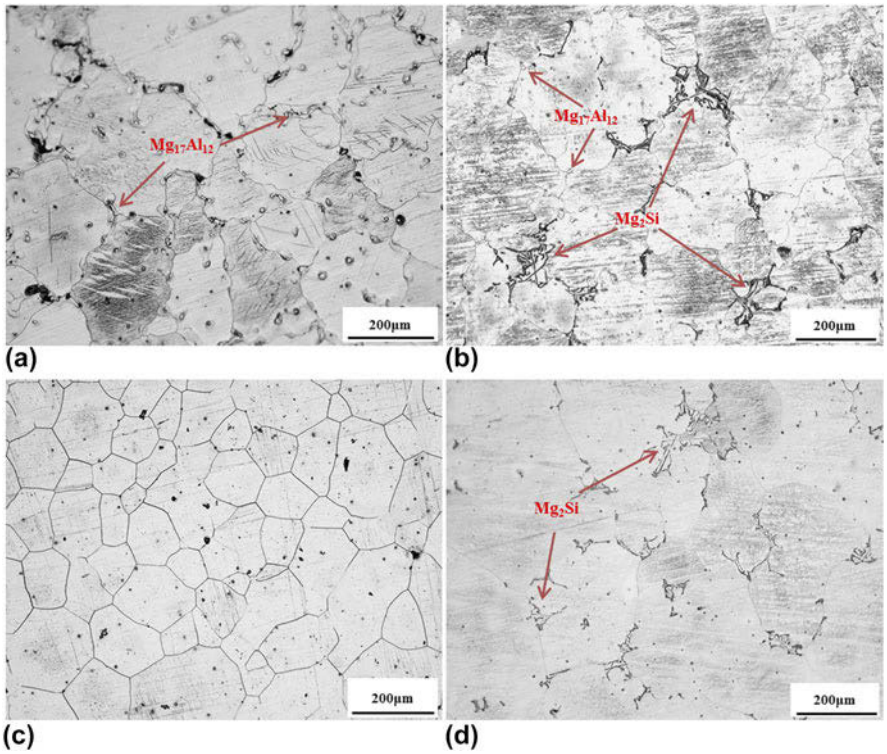

FIG. 2. Optical micrographs of Mg–3Al–Zn [(a) as-cast and (c) homogenized] and Mg–3(Al–Si)–Zn [(b) as-cast and (d) homogenized].

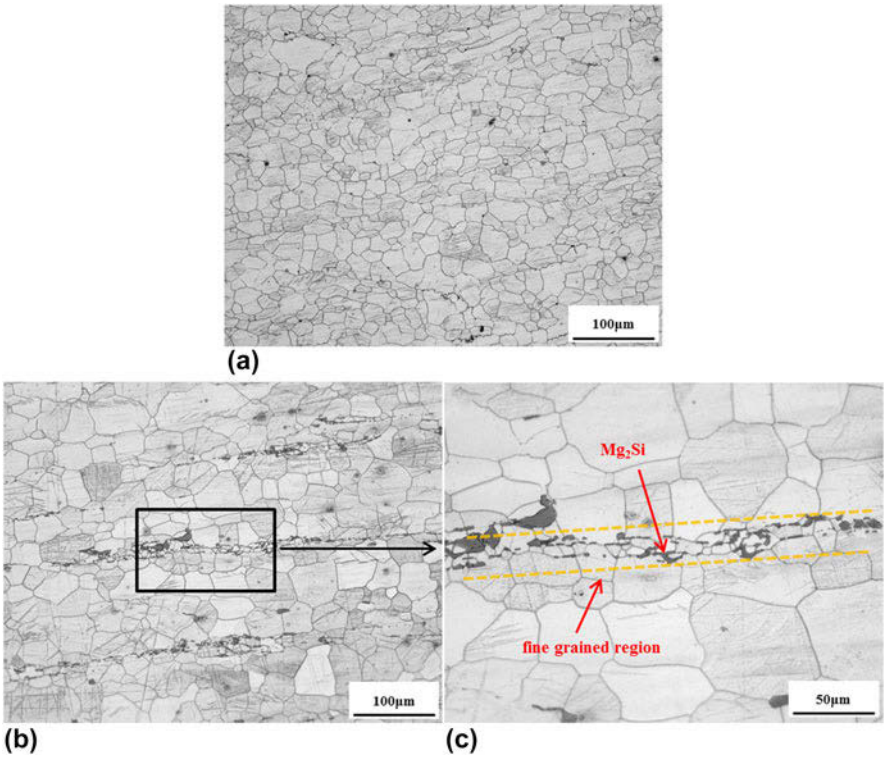

FIG. 3. Optical micrographs of as-extruded Mg–3Al–Zn (a) and Mg–3(Al–Si)–Zn (b, c) alloys.

particle-stimulated nucleation (PSN).[28] However, the hard and brittle Mg_2Si phases were fragmented during hot extrusion, which produces the effect of a shear cut on the matrix grains and contributes to grain refinement further.

The as-extruded alloys were subjected to hot rolling process at 400 °C with a total reduction of ~73%. Figure 4 shows the microstructures and grain size distribution of the as-rolled Mg–3Al–Zn and Mg–3(Al–Si)–Zn alloys. The microstructures in both as-rolled Mg–3Al–Zn and Mg–3(Al–Si)–Zn alloys consist of duplex grain structures including coarse grain regions (≥15 μm) and fine grain regions (<15 μm). It is obvious that more ultra-fine grains were obtained in the fine grain regions of the Mg–3(Al–Si)–Zn alloy with the Al–Si eutectic compared to the Mg–3Al–Zn alloy, as shown in Figs. 4(a) and 4(b). This bimodal grain size distribution and corresponding grain size values were given in Figs. 4(c) and 4(d). The obtained microstructures were analyzed according to the area-based averaging method[23]:

$$\bar{d}_{\mathrm{m}} = \left(A_{\mathrm{f}}/d_{\mathrm{fm}}^2 + A_{\mathrm{c}}/d_{\mathrm{cm}}^2\right)^{-1/2} \quad , \qquad (1)$$

where d_{m} represents the overall average grain size, A_{f} and A_{c} represent the area fractions of fine grains and coarse grains, respectively, and d_{fm} and d_{cm} are the average grain sizes of the fine grain and coarse grain regions, respectively. More microstructural details of this method are presented in Ref. 23.

The grain size distributions of both alloys exhibit distinct bimodal distribution characteristics. The duplex grain microstructure of the Mg–3Al–Zn alloy with an average grain size of ~9.7 μm involves a 44% area fraction of coarse grains with a size of ~34 μm. However, the microstructure of the Mg–3(Al–Si)–Zn alloy exhibits a significant refinement with an average grain size of ~4.5 μm, but it contains more than 50% area fraction of coarse grains with a size of ~23 μm and approximately 43% area fraction of fine grains with a size smaller than 5 μm. Jiang et al.[17] suggested that twinning and DRX play a predominant role in different stages of plastic deformation. Twins more easily appear at the initial stage of the hot rolling deformation. However, as the rolling process continues, the newly formed fine grains generally nucleate at the grain boundaries during DRX, and the growth of the DRX grains is restricted because of the pinning effect of the second phase particles. This eventually leads to the formation of a double scale microstructure. The dual-scale microstructure that is composed of coarse deformed grains and newly formed fine grains was also reported by Park et al.[29]

B. Dynamic recrystallization behavior

DRX plays an important role in grain refinement and improvement in mechanical properties for magnesium alloys during plastic deformation.[30] Figure 5 exhibits the microstructures and second phase distribution of the

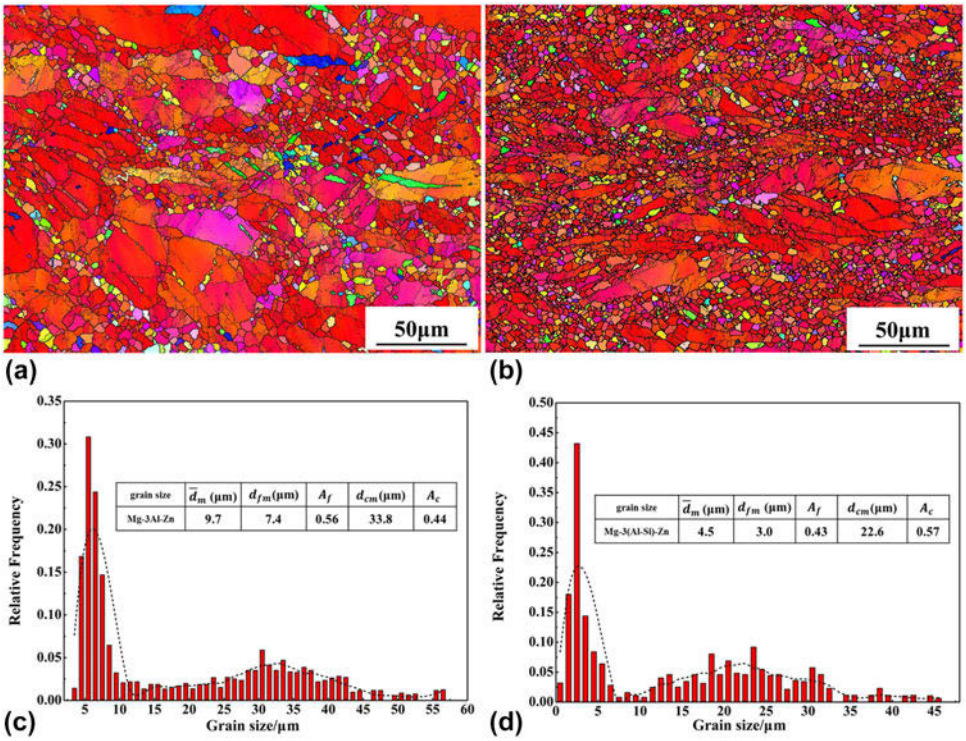

FIG. 4. EBSD images and grain size distribution of as-rolled Mg–3Al–Zn (a, c) and Mg–3(Al–Si)–Zn (b, d) alloys.

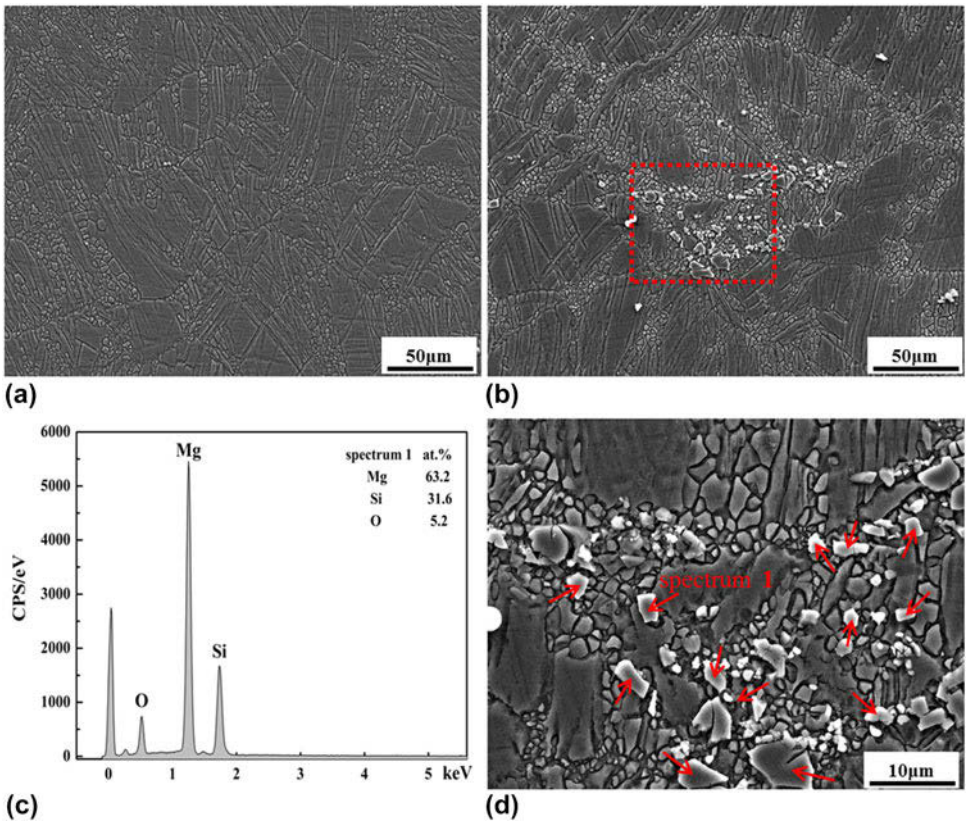

FIG. 5. SEM microstructure of as-rolled Mg–3Al–Zn (a) and Mg–3(Al–Si)–Zn alloy (b, d) and energy spectrum (c) of Mg_2Si in partial magnification image (d).

as-rolled Mg–3Al–Zn and Mg–3(Al–Si)–Zn alloys. It can be seen clearly that both alloys shows a typical bimodal distribution after rolling deformation including fine-grained area and coarse-grained area as shown in Figs. 5(a) and 5(b). Compared with Fig. 5(a), it can be seen from Fig. 5(b) that the proportion of fine grain area is improved obviously and Mg_2Si second phase segregation around the fine grain area. It is noteworthy that the fine grain area around the Mg_2Si second phase in Fig. 5(b) seems to be larger and the grain size is finer than that in Fig. 5(a). Therefore, the Mg_2Si particles could have great effect on fine grain area around themselves. To analyze the fine-grained region with more Mg_2Si particles in Fig. 5(b), the rectangular area in Fig. 5(b) is magnified, as shown in Fig. 5(d). Combined with the energy spectrum analysis of Fig. 5(c), it can be confirmed that the second phase particles in Fig. 5(d) are Mg_2Si phase, as indicated by red arrows. The effect of Mg_2Si particles on grain refinement can be described from two aspects: on one hand, as reported by Robson et al.,[31] large Mg_2Si particles ($\geq$1 μm in diameter) could stimulate nucleation for recrystallization via a PSN mechanism. This could be related to the sub-boundary migration that appears around large hard particles in the deformed region during hot rolling, leading to lattice rotation, a misorientation gradient and the formation of a new grain nucleus that can grow a recrystallized grain[32]; on the other hand, fine Mg_2Si particles ($<$1 μm in diameter) could inhibit the new recrystallization grain growth though pinning grain boundaries, hindering grain boundaries and dislocation movement.[28]

To investigate the effect of texture and PSN on DRX behavior, the (0002) pole figures, recrystallized microstructure and frequency distribution histograms are shown in Fig. 6. Both alloys showed a typical strong basal texture along the *c*-axis, parallel to the ND, in the vast majority of the grains during the hot rolling process. It has been reported[33] that a strengthening basal texture, in which the *c*-axis of most of the grains is parallel to ND, forces most of the grains to present a hard orientation with a smaller Schmid factor of basal $\langle a \rangle$ slip, which results in an increase in yield stress. Thus, weakening of the basal texture can lead to a decrease in the yield strength. Compared to the as-rolled Mg–3Al–Zn alloy, the alloy with the Al–Si eutectic exhibited a weakened base texture with an intensity decrease from 19.4 to 11.4, as shown in Figs. 6(a) and 6(b). Compared to the recrystallized microstructure and frequency distribution histograms of the Mg–3Al–Zn alloy sheet, as shown in Figs. 6(c) and 6(e), the Mg–3(Al–Si)–Zn alloy after hot

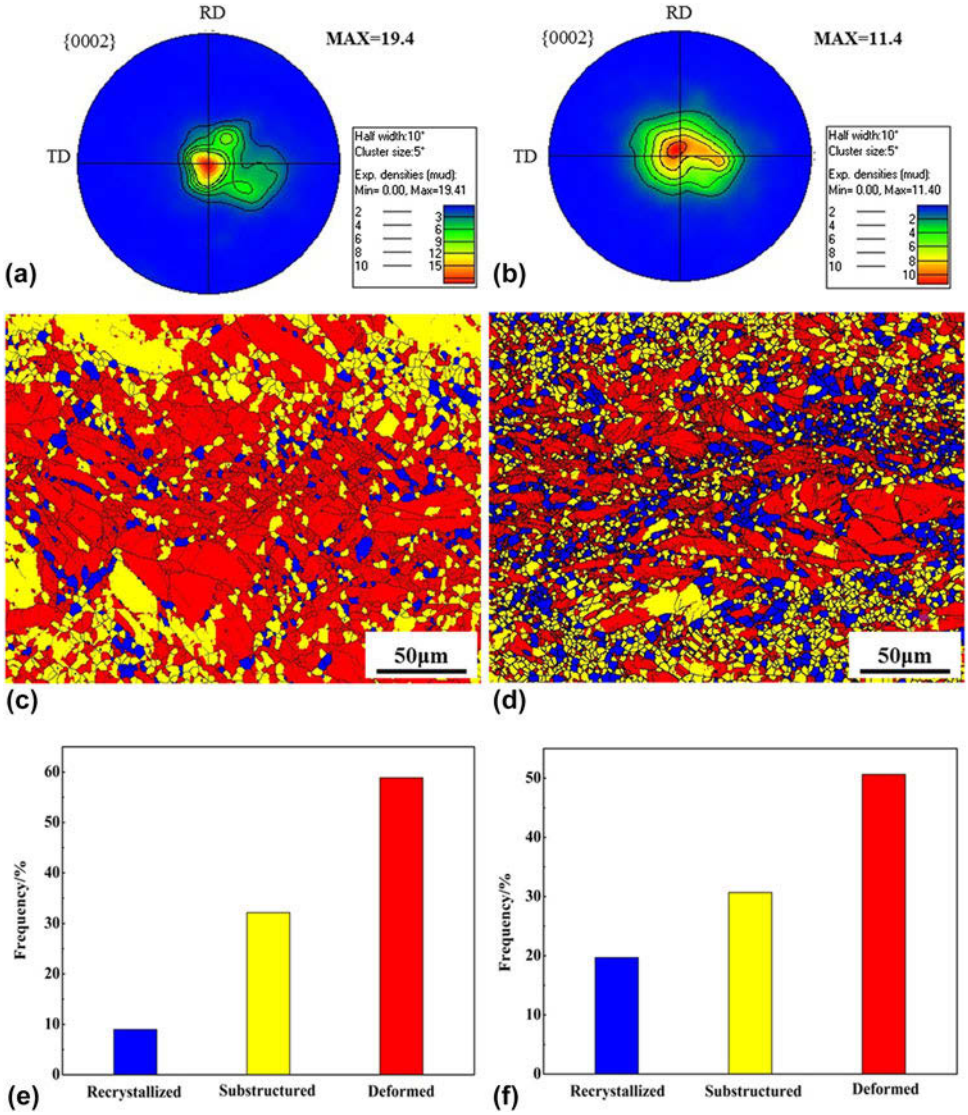

FIG. 6. The {0002} pole figures and recrystallized microstructure and frequency distribution of as-rolled Mg–3Al–Zn (a, c, e) and Mg–3(Al–Si)–Zn (b, d, f).

rolling contains a higher percentage of recrystallized and substructure regions. The frequency of completely recrystallized regions for Mg–3(Al–Si)–Zn increased from ~10% to ~20% compared to Mg–3Al–Zn. Moreover, Figs. 6(c) and 6(d) show finer recrystallized grain regions surrounded by some coarse substructure and deformed grains.

The deformed and substructure grains have elongated along the roll direction, as shown in Figs. 4, 5, and 6. During hot rolling, the grains with a basal slip orientation will adapt to the plastic strain and elongate because of the relatively lower critical resolved shear stress (CRSS) of merely 2–4 MPa for the basal slip.[6,30] Dynamic recrystallization dissipates the strain energy and releases the stress concentration accompanied by activation of the nonbasal slip, e.g., prismatic slip and pyramidal slip systems at elevated temperatures.[19,30,32] The lower fraction of recrystallization compared to the deformation and substructure could be attributed to the relatively limited storage ability of plastic strain energy.[28] The effect of Mg_2Si particles on the Mg–3(Al–Si)–Zn alloy could be that more nucleation sites were generated for recrystallization, and the new grains growing with various orientations departed from the basal texture.[34] This could also explain the decrease in the basal texture upon the addition of the Al–Si eutectic, as shown in Figs. 6(a) and 6(b). It is possible that the new grains generated by PSN with DRX behavior show some growth restrictions that are different from other recrystallization mechanisms, such as shear band nucleation[31] and deformation twin nucleation.[32] Accordingly, it is necessary to investigate the microtexture of the finer recrystallized regions and the effect of

the recrystallized texture and PSN mechanism on the mechanical properties and plastic forming ability of the alloy.

C. Mechanical properties

The representative tensile true stress–strain curves at room temperature for the as-rolled alloy with four different components and the values for the yield strength, UTS, and elongation to fracture for the studied alloys are shown in Fig. 7. All the specimens showed a continuous work hardening behavior until fracture. As shown in Fig. 7(a), with the addition of the Al–Si eutectic, the UTS, elongation to fracture, and yield strength of the Mg–3(Al–Si) alloy increased compared to the Mg–3Al alloy created under the same thermal mechanical forming technology. This indicates that a proper addition method for Si, such as the addition of an Al–Si eutectic alloy, might be beneficial for AZ series alloys if accompanied by conventional plastic deformation. A similar trend can also be observed for the as-rolled Mg–3(Al–Si)–Zn alloy. However, the elongation to fracture of the Mg–3(Al–Si)–Zn alloy is slightly decreased compared to the Mg–3Al–Zn alloy under the same treatment. Specifically, the Mg–3(Al–Si)–Zn alloy sheet shows an increase in the UTS from 330 to 367 MPa and a decrease in the elongation from 12.5% to 12%. However, the change in yield strength was not noticeable.

Figure 8 shows the tensile fracture surfaces of as-rolled Mg–3Al–Zn and Mg–3(Al–Si)–Zn alloy sheets. The tensile fracture surfaces of as-rolled Mg–3Al–Zn specimen exhibit more ductile fracture characteristics with a large amount of dimples distribute higher density in α-Mg matrix, as shown in Fig. 8(a). The fracture features of as-rolled Mg–3(Al–Si)–Zn specimen assume the features of a little cleavage fracture, in which more cleavage facets and tearing ridge could be observed, compared with that of Mg–3Al–Zn. Furthermore, it should be noticed that some Mg_2Si particles can be found in the tensile fracture surfaces of Mg–3(Al–Si)–Zn specimen as shown in Fig. 8(b). It is helpful for understanding the reason for the slight decrease of elongation due to the cut apart effect of Mg_2Si particles on Mg matrix.

Liang et al.[20] have studied the relationship between mechanical properties and texture distribution of AZ31 magnesium alloy during conventional rolling process, and also acquired enhancement mechanical properties with the yield strength of ~180 MPa and the tensile

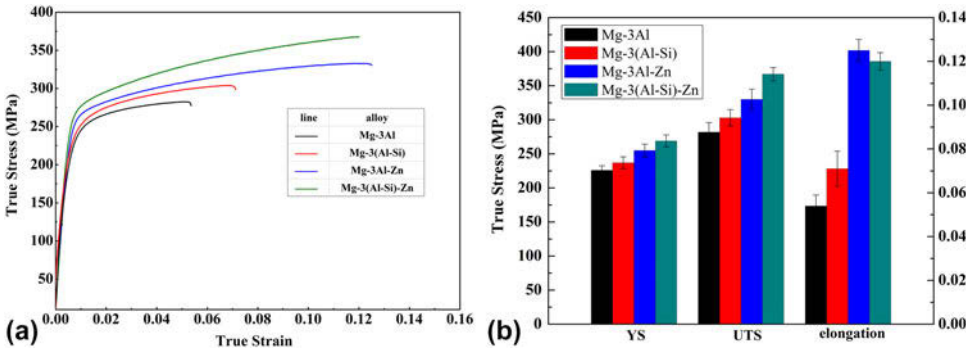

FIG. 7. True stress–strain curves (a) and histograms of tensile properties (b) of as-rolled alloys.

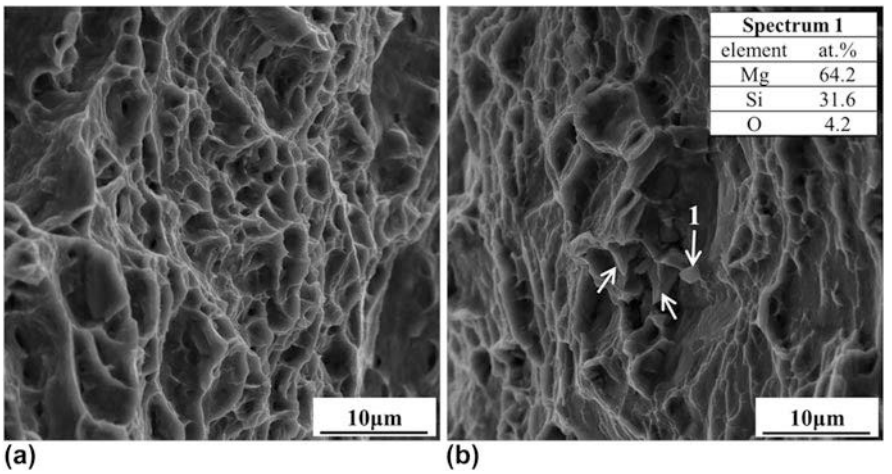

FIG. 8. Tensile fracture surfaces of as-rolled Mg–3Al–Zn (a) and Mg–3(Al–Si)–Zn (b) alloy sheets.

strength of ~270 MPa. In this study, although the basal texture is weakened by the DRX, the tensile strength is obviously improved. This improvement in the mechanical properties can be attributed to grain refinement in both fine grain and coarse grain regions, as shown in Figs. 4, 5, and 6. The yield strength of Mg–3(Al–Si)–Zn alloy with the addition of Al and Si using an Al–Si eutectic does not exhibit an obvious change, but the UTS increased remarkably compared to the Mg–3Al–Zn alloy, as shown in Fig. 7(b). This can be attributed to the effective grain refinement caused by DRX in the as-rolled Mg–3(Al–Si)–Zn alloy and second phrase strengthening caused by the broken Mg_2Si particles, although the basal texture is weakened in the Mg–3(Al–Si)–Zn alloy sheet, as shown in Fig. 6. As a result, the improved tensile strength of the Mg–3(Al–Si)–Zn alloy upon the addition of the Al–Si eutectic can be generally explained as the competition of two opposite effects: one is the softening effect due to the weakened basal texture, and the other is the strengthening effect of grain refinement. This results form the PSN on recrystallization, which plays a dominant role in the present work.

IV. CONCLUSIONS

A suitable alloying method combined with a conventional hot rolling process was used to produce AZ31 alloy sheets with enhanced mechanical properties. The mechanical properties, microstructure evolution, and dynamic recrystallization mechanism were investigated. The primary conclusions are as follows:

(1) The microstructures of both the Mg–3Al–Zn and Mg–3(Al–Si)–Zn alloy sheets exhibit a duplex grain structure after hot rolling that includes coarse grains and fine grains. The Mg–3(Al–Si)–Zn alloy sheet with the addition of the Al–Si eutectic presents a remarkable grain refinement in the fine grain and coarse grain regions compared to the Mg–3Al–Zn sheet.

(2) The fragmented, refined Mg_2Si particles play a key role in providing potential nucleation sites for recrystallization in the as-rolled Mg–3(Al–Si)–Zn alloy sheet with the Al–Si eutectic through PSN.

(3) The Mg–3(Al–Si)–Zn alloy sheet shows more completely recrystallized regions and a weakened basal texture, which are in agreement with superior grain refinement. The weakened basal texture could be attributed to recrystallized new grains growing with various orientations that depart from the basal texture.

(4) Both the yield strength and the UTS of the Mg–3(Al–Si)–Zn alloy with the Al–Si eutectic were improved compared to the Mg–3Al–Zn alloy under the same treatment. This can be attributed to the competition between the softening effect due to the weakened basal texture and the strengthening effect of the grain refinement.

ACKNOWLEDGMENTS

This work was financially supported by "National Natural Science Foundation of China" (Grant Nos. 51175363, 51274149 and 51474152).

REFERENCES

1. H. Zhang, G. Huang, H.J. Roven, L. Wang, and F. Pan: Influence of different rolling routes on the microstructure evolution and properties of AZ31 magnesium alloy sheets. *Mater. Des.* **50**, 667 (2013).
2. N.G. Ross, M.R. Barnett, and A.G. Beer: Effect of alloying and extrusion temperature on the microstructure and mechanical properties of Mg–Zn and Mg–Zn–RE alloys. *Mater. Sci. Eng., A* **619**, 238 (2014).
3. H. Huang, G.Y. Yuan, Z.H. Chu, and W.J. Ding: Microstructure and mechanical properties of double continuously extruded Mg–Zn–Gd-based magnesium alloys. *Mater. Sci. Eng., A* **560**, 241 (2013).
4. W.L. Chen, W.W. Wang, H.X. Wang, Y.M. Ling, and S.H. Park: Improved mechanical properties of ECAPed Mg–15Al alloy through Nd addition. *Mater. Sci. Eng., A* **633**, 63 (2015).
5. N. Stanford, R.K.W. Marceau, and M.R. Barnett: The effect of high yttrium solute concentration on the twinning behavior of magnesium alloys. *Acta Mater.* **82**, 447 (2015).
6. D. Ando, J. Koike, and Y. Sutou: The role of deformation twinning in the fracture behavior and mechanism of basal textured magnesium alloys. *Mater. Sci. Eng., A* **600**, 145 (2014).
7. K.B. Nie, K.K. Deng, X.J. Wang, F.J. Xu, K. Wu, and M.Y. Zheng: Multidirectional forging of AZ91 magnesium alloy and its effects on microstructures and mechanical properties. *Mater. Sci. Eng., A* **624**, 157 (2015).
8. G.Y. Yuan, Z.L. Liu, Q.D. Wang, and W.J. Ding: Microstructure refinement of Mg–Al–Zn–Si alloys. *Mater. Lett.* **56**, 53 (2002).
9. F. Xue, X.G. Min, and Y.S. Sun: Microstructures and mechanical properties of AZ91 alloy with combined additions of Ca and Si. *J. Mater. Sci.* **41**, 4725 (2006).
10. W. Guo, Q.D. Wang, B. Ye, and H. Zhou: Enhanced microstructure homogeneity and mechanical properties of AZ31–Si composite by cyclic closed-die forging. *J. Alloys Compd.* **552**, 409 (2013).
11. W.H. Wang, H.X. Wang, Y.M. Liu, H.H. Nie, and W.L. Chen: Effect of SiC nanoparticles addition on the microstructures and mechanical properties of ECAPed Mg9Al–1Si alloy. *J. Mater. Res.* **32**, 615 (2017). doi: 10.1557/jmr.2016.514.
12. Z.W. Wang, H.X. Wang, J.L. Gong, M. Li, W.L. Cheng, and W. Liang: Modification and refinement effects of Sb and Sr on $Mg_{17}Al_{12}$ and Mg_2Si phases in Mg–12Al–0.7Si alloy. *China Foundry* **13**, 310 (2016).
13. S.D. Sheng, D. Chen, and Z.H. Chen: Effects of Si addition on microstructure and mechanical properties of RS/PM (rapid solidification and powder metallurgy) AZ91 alloy. *J. Alloys Compd.* **470**, L17 (2009).
14. Y.Z. Lü, Q.D. Wang, X.Q. Zeng, Y.P. Zhu, and W.J. Ding: Behavior of Mg–6Al–*x*Si alloys during solution heat treatment at 420 °C. *Mater. Sci. Eng., A* **301**, 255 (2001).
15. Q.X. Shi, L.P. Bian, W. Liang, Z.Q. Chen, F.Q. Yang, and Y.D. Wang: Effects of adding Al–Si eutectic alloy and hot rolling on microstructures and mechanical behavior of Mg–8Li alloys. *J. Alloys Compd.* **631**, 129 (2015).
16. J.L. Gong, W. Liang, H.X. Wang, X.G. Zhao, and L.P. Bian: Microstructure and mechanical properties of Mg–12Al–0.7Si magnesium alloy processed by equal channel angular pressing. *Rare Met. Mater. Eng.* **42**, 1800 (2013).
17. M.G. Jiang, H. Yan, and R.S. Chen: Enhanced mechanical properties due to grain refinement and texture modification in an AZ61 Mg alloy processed by small strain impact forging. *Mater. Sci. Eng., A* **621**, 204 (2015).

18. M.G. Jiang, H. Yan, and R.S. Chen: Microstructure, texture and mechanical properties in an as-cast AZ61 Mg alloy during multi-directional impact forging and subsequent heat treatment. *Mater. Des.* **87**, 891 (2015).
19. S.Q. Zhu, H.G. Yan, J.H. Chen, Y.Z. Wu, J.Z. Liu, and J. Tian: Effect of twinning and dynamic recrystallization on the high strain rate rolling process. *Scr. Mater.* **63**, 985 (2010).
20. Z.W. Wang, H.X. Wang, W.H. Wang, G.X. Ren, K.B. Nie, Y.M. Liu, and W. Liang: The effect of high Al content on the microstructure and mechanical properties of Mg–*x*Al alloys. *Int. J. Mater. Res.* **108**, 45 (2017).
21. M.T. Perez-Prado, J.A. del Valle, and O.A. Ruano: Grain refinement of Mg–Al–Zn alloys via accumulative roll bonding. *Scr. Mater.* **51**, 1093 (2004).
22. X.L. Wu, M.X. Yang, F.P. Yuan, G.L. Wu, Y.J. Wei, X.X. Huang, and Y.T. Zhu: Heterogeneous lamella structure unites ultrafine-grain strength with coarse-grain ductility. *Proc. Natl. Acad. Sci. U. S. A.* **112**, 14501 (2015).
23. W.Z. Chen, Y. Yu, X. Wang, E.D. Wang, and Z.Y. Liu: Optimization of rolling temperature for ZK61 alloy sheets via microstructure uniformity analysis. *Mater. Sci. Eng., A* **575**, 136 (2013).
24. H. Yan, Y.S. Rao, and R. He: Morphological evolution of semi-solid Mg_2Si/AM60 magnesium matrix composite produced by ultrasonic vibration process. *J. Mater. Process. Technol.* **214**, 612 (2014).
25. S. Fintová and L. Kunz: Fatigue properties of magnesium alloy AZ91 processed by severe plastic deformation. *J. Mech. Behav. Biomed. Mater.* **42**, 219 (2015).
26. Q. Guo, H.G. Yan, Z.H. Chen, and H. Zhang: Grain refinement in as-cast AZ80 Mg alloy under large strain deformation. *Mater. Charact.* **58**, 162 (2007).
27. H.X. Wang, B. Zhou, Y.T. Zhao, K.K. Zhou, W.L. Cheng, and W. Liang: Effect of Si addition on the microstructure and mechanical properties of ECAPed Mg–15Al alloy. *Mater. Sci. Eng., A* **589**, 119 (2014).
28. T. Al-Samman: Modification of texture and microstructure of magnesium alloy extrusions by particle-stimulated recrystallization. *Mater. Sci. Eng., A* **560**, 561 (2013).
29. S.H. Park, S.H. Kim, Y.M. Kim, and B.S. You: Improving mechanical properties of extruded Mg–Al alloy with a bimodal grain structure through alloying addition. *J. Alloys Compd.* **646**, 932 (2015).
30. N. Stanford and M.R. Barnett: The origin of "rare earth" texture development in extruded Mg-based alloys and its effect on tensile ductility. *Mater. Sci. Eng., A* **496**, 399 (2008).
31. J.D. Robson, D.T. Henry, and B. Davis: Particle effects on recrystallization in magnesium–manganese alloys: Particle-stimulated nucleation. *Acta Mater.* **57**, 2739 (2009).
32. I. Basu and T. Al-Samman: Twin recrystallization mechanisms in magnesium-rare earth alloys. *Acta Mater.* **96**, 111 (2015).
33. X.S. Huang, K. Suzuki, and N. Saito: Textures and stretch formability of Mg–6Al–1Zn magnesium alloy sheets rolled at high temperatures up to 793 K. *Scr. Mater.* **60**, 651 (2009).
34. X.S. Huang, K. Suzuki, Y. Chino, and M. Mabuchi: Influence of initial texture on cold deep draw ability of Mg–3Al–1Zn alloy sheets. *Mater. Sci. Eng., A* **565**, 359 (2013).